Centralized Neural Identification and Indirect Adaptive I-term Control of Distributed Parameter Bioprocess Plant*

I.Baruch, E. Echeverria Salidierna, B. Nenkova

Key Words: *Recurrent neural network model; Levenberg-Marquardt learning; system identification and state estimation; indirect adaptive neural control; distributed parameter anaerobic bioprocess plant.*

Abstract. *The paper proposes a Recurrent Neural Network (RNN) topology and a recursive Levenberg-Marquardt (L-M) algorithm of its learning capable to estimate the states and parameters of an anaerobic continuous bioprocess plant in noisy environment. The analytical model of the digestion bioprocess represents a distributed parameter system, which is reduced to a lumped system using the orthogonal collocation method, applied in four collocation points. The proposed RNN identifier is incorporated in an indirect adaptive control scheme (sliding mode and optimal control) containing also an integral term. The proposed control scheme is applied for real-time identification and control of continuous fixed bad and recirculation tank bioreactor model in five points, taken from the literature, where a fast convergence, noise filtering and low mean squared error of reference tracking were achieved*

1. Introduction

In last decade, the Artificial Neural Networks (ANNs) have been widely employed to dynamic process modeling, identification, prediction and control, [1-9]. Many applications have been done for identification and control of biotechnological plants too, [6], [10-12], [14-16]. Among several possible NN architectures the ones most widely used are the Feedforward NN (FFNN) and the Recurrent NN (RNN), [1]. The main NN property namely the ability to approximate complex non-linear relationships without prior knowledge of the model structure makes them a very attractive alternative to the classical modeling and control techniques. Also, a great boost has been made in the design of NN-based adaptive control incorporating integral plus state control action in the control law, [12]. The FFNN and the RNN have been applied for Distributed Parameter Systems (DPS) identification and control too, [2-9], [15]. Unfortunately, all these works suffered of the same inconvenience, that the FFNNs used are of higher dimension having great complexity which made difficult their application. In [10-14], a new canonical Recurrent Trainable NN (RTNN) architecture, and a dynamic Backpropagation (BP) learning algorithm has been applied for systems identification and control of nonlinear plants with equal input/output dimensions, obtaining good results. In the present paper, this RTNN model will be used for identification, and indirect control, of a digestion anaerobic DPS [6], [15], modeled by PDE/ODE, and simplified using the Orthogonal Collocation Method (OCM) in four collocation points of the fixed bed and one more- for the recirculation tank. Here the BP learning is changed by the Levenberg Marquardt (L-M) one, [16]. This DPS nonlinear plant, described by ODE, has excessive high-dimensional measurements which means that the plant output dimension is greater than the plant control input one (rectangular system), requiring special reference choice, representing a data fusion technique. Here, the used control laws are extended with an I-term, representing an I-plus state action, capable to speed up the systems reaction and to augment its resistance to noise.

** This paper is submitted for possible publication in the journal "Information Technologies and Control".*

2. Description of the RTNN Topology and Learning

RTNN topology and BP learning. Block-diagrams of the RTNN topology and its adjoint are given on *figure 1*, and *figure 2*.

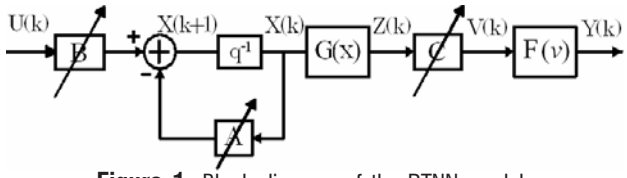

Figure 1. Block diagram of the RTNN model

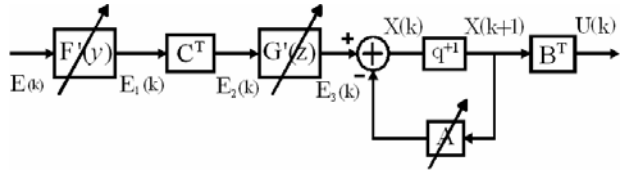

Figure 2. Block diagram of the adjoint RTNN model

Following *figure 1*, and *figure 2*, we could derive the dynamic BP algorithm of its learning based on the RTNN topology using the diagrammatic method of [17]. The RTNN topology and BP learning are described by the following equations:

(1) $X(k+1) = AX(k) + BU(k)$; $B = [B_1 ; B_0]$;

(2) $Z_1(k) = G[X(k)]$; $U^T = [U_1 ; U_2]$;

(3) $V(k) = CZ(k)$; $C = [C_1 ; C_0]$; $Z^T = [Z_1 ; Z_2]$;

(4) $Y(k) = F[V(k)]$; $E(k) = T(k)-Y(k)$;

(5) $A = \text{block-diag}(Ai)$, $|Ai| < 1$;

(6) $W(k+1) = W(k) + \eta\, \Delta W(k) + \alpha\, \Delta W_{ij}(k-1)$;

(7) $E_1(k) = F'[Y(k)]\, E(k)$; $F'[Y(k)] = [1-Y^2(k)]$;

(8) $\Delta C(k) = E_1(k)\, Z^T(k)$;

(9) $E_3(k) = G'[Z(k)]\, E_2(k)$; $E_2(k) = C^T(k)\, E_1(k)$;

(10) $\Delta B(k) = E_3(k)\, U^T(k)$; $G'[Z(k)] = [1-Z^2(k)]$;

(11) $\Delta A(k) = E_3(k)\, X^T(k)$;

(12) $Vec(\Delta A(k)) = E_3(k) \cdot X(k)$,

where X, Y, U are state, augmented output, and input vectors with dimensions N, (L+1), (M+1), respectively, where Z_1 and U_1 are the (Nx1) output and (Mx1) input of the hidden layer; the constant scalar threshold entries are $Z_2 = -1$, $U_2 = -1$, respectively; V is a (Lx1) pre-synaptic activity of the output layer; T is the (Lx1) plant output vector, considered as a RNN reference; A is (NxN) block-diagonal weight matrix; B and C are [Nx(M+1)] and [Lx(N+1)]- augmented weight matrices; B_0 and C_0 are (Nx1) and (Lx1) threshold weights of the hidden and output layers; F[.], G[.] are vector-valued tanh(.)-activation functions with corresponding dimensions; F'[.], G'[.] are the derivatives of these tanh(.) functions; W is a general weight, denoting each weight matrix (C, A, B) in the RTNN model, to be updated; ΔW (ΔC, ΔA, ΔB), is the weight correction of W; η, α are learning rate parameters; ΔC is an weight correction of the learned matrix C; ΔB is an weight correction of the learned matrix B; the diagonal of the matrix A is denoted by Vec(.) and equation (12) represents its learning as an element-by-element vector products; E, E_1, E_2, E_3, are error vectors with appropriate dimensions, predicted by the adjoint RTNN model, given on *figure 2*. The stability of the RTNN model is assured by the activation functions (-1, 1) bounds and by the local stability weight bound condition, given by (5).

Theorem of stability of RTNN as system identifier. Let the RTNN with Jordan Canonical Structure is given by equations (1)-(5) (see *figure 1*) and the nonlinear plant model, is as follows:

$$X_d(k+1) = f[X_d(k), U(k)];$$
$$Y_d(k) = g[X_d(k)],$$

where $\{Y_d(.), X_d(.), U(.)\}$ are output, state and input variables with dimensions L, N_d, M, respectively; f(.), g(.) are vector valued nonlinear functions with respective dimensions. Under the assumption of RTNN identifiability made, the application of the BP learning algorithm for A(.), B(.), C(.),described by equation (24)-(31), and the learning rates $\eta(k)$, $\alpha(k)$ (considered as time-dependent and normalized with respect to the error) are derived using the following Lyapunov function:

$$L(k) = L_1(k) + L_2(k),$$

where $L_1(k)$ and $L_1(k)$ are given by

$$L_1(k) = \tfrac{1}{2} e^2(k);$$
$$L_2(k) = tr(\tilde{W}_A(k)\tilde{W}_A^T(k)) + tr(\tilde{W}_B(k)\tilde{W}_B^T(k)) + tr(\tilde{W}_C(k)\tilde{W}_C^T(k)),$$

where

$$\tilde{W}_A(k) = \hat{A}(k) - A^*, \tilde{W}_B(k) = \hat{B}(k) - B^*, \tilde{W}_C(k) = \hat{C}(k) - C^*.$$

Are vectors of the estimation error, and the system weights (A^*, B^*, C^*), and $(\hat{A}(k), \hat{B}(k), \hat{C}(k))$ denoted the ideal neural weight and the estimate of the neural weight at the k-th step, respectively, for each case. Then the identification error is bounded, i.e.

$$L(k+1) = L_1(k+1) + L_2(k+1);$$
$$\Delta L(k+1) = L(k+1) - L(k) < 0,$$

where the condition for $\Delta L_1(k+1)<0$ is that

$$\frac{\left(1-\frac{1}{\sqrt{2}}\right)}{\psi_{max}} < \eta_{max} < \frac{\left(1+\frac{1}{\sqrt{2}}\right)}{\psi_{max}}.$$

And for $\Delta L_2(k+1)<0$ we have

$$\Delta L_2(k+1) < -\eta_{max}|e(k+1)|^2 - \alpha_{max}|e(k)|^2 + d(k+1).$$

Note that η_{max} changes adaptively during the RTNN learning and $\eta_{max} = \max_{i=1}^{3}\{\eta_i\}$.

Where all: the unmodeled dynamics, the approximation errors and the perturbations, are represented by the d-term. The Rate of Convergence Lemma completed the proof.

Rate of convergence Lemma. Let ΔL_2 is defined. Then, applying the limit's definition, the identification error bound condition is obtained as

$$\overline{\lim_{k\to\infty}} \frac{1}{k}\sum_{t=1}^{k}\left(|E(t)|^2 + |E(t-1)|^2\right) \le d.$$

Proof: Starting from the final result of the theorem of RTNN stability

$$\Delta L(k) \le -\eta(k)|E(k)|^2 - \alpha(k)|E(k-1)|^2 + d$$

and iterating from k=0, we get

$$L(k+1) - L(0) \le -\sum_{t=1}^{k}|E(t)|^2 - \sum_{t=1}^{k}|E(t-1)|^2 + dk;$$

$$\sum_{t=1}^{k}\left(|E(t)|^2 + |E(t-1)|^2\right) \le dk - L(k+1) + L(0) \le dk + L(0).$$

From here, we could see that *d* must be bounded by weight matrices and learning parameters, in order to obtain: $\Delta L(k) \in L(\infty)$.

As a consequence, we obtained: $A(k) \in L(\infty)$, $B(k) \in L(\infty)$, $C(k) \in L(\infty)$.

The Rate of Convergence Lemma used is given in [13]. The complete proof of that Theorem of stability is given in [11].

Recursive Levenberg-Marquardt learning. The general recursive L-M algorithm of learning, [16] is given by the following equations:

(13) $W(k+1) = W(k) + P(k)\nabla Y[W(k)]E[W(k)]$;

(14) $Y[W(k)] = g[W(k), U(k)]$;

(15) $E^2[W(k)] = \{Y_p(k) - g[W(k), U(k)]\}^2$;

(16) $DY[W(k)] = \frac{\partial}{\partial W} g[W, U(k)]\Big|_{W=W(k)}$,

where W is a general weight matrix (A, B, C) under modification; P is the covariance matrix of the estimated weights updated; DY[.] is an nw-dimensional gradient vector; Y is the RTNN output vector which depends of the updated weights and the input; E is an error vector; Yp is the plant output vector, which is in fact the target vector. Using the same RTNN adjoint

block diagram (see *figure 2*), it was possible to obtain the values of the gradients DY[.] for each updated weight, propagating the value D(k) = I through it. Applying equation (16) for each element of the weight matrices (A, B, C) in order to be updated, the corresponding gradient components are as follows:

(17) $DY[C_{ij}(k)] = D_{1,i}(k) Z_j(k)$;

(18) $D_{1,i}(k) = F_i'[Y_i(k)]$;

(19) $DY[A_{ij}(k)] = D_{2,i}(k) X_j(k)$;

(20) $DY[B_{ij}(k)] = D_{2,i}(k) U_j(k)$;

(21) $D_{2,i}(k) = G_i'[Z_i(k)] C_i D_{1,i}(k)$.

The P(k) matrix was computed recursively by the equation

(22) $P(k) = \alpha^{-1}(k)\{P(k-1) - P(k-1)\Omega[W(k)] S^{-1}[W(k)]\Omega^T[W(k)]P(k-1)\}$,

where the S(.), and Ω(.) matrices were given as follows:

(23) $S[W(k)] = \alpha(k)\Lambda(k) + \Omega^T[W(k)]P(k-1)\Omega[W(k)]$;

$$\Omega^T[W(k)] = \begin{bmatrix} & \nabla Y^T[W(k)] & \\ 0 \;\; \mathrm{L} & 1 & \mathrm{L} \;\; 0 \end{bmatrix};$$

(24) $$\Lambda(k)^{-1} = \begin{bmatrix} 1 & 0 \\ 0 & \rho \end{bmatrix}; 10^{-4} \le \rho \le 10^{-6};$$

$$0.97 \le \alpha(k) \le 1; 10^3 \le P(0) \le 10^6$$

The matrix Ω(.) had a dimension (Nwx2), whereas the second row had only one unity element (the others were zero). The position of that element was computed by

(25) $i = k \bmod(Nw) + 1;\ k > Nw.$

After this, the given up topology and learning will be applied for an anaerobic wastewater distributed parameter centralized system identification and I-term control.

3. Indirect Adaptive Neural Control with I-term

Sliding mode control with I-term. The block-diagram of the control system is given on *figure 3*.

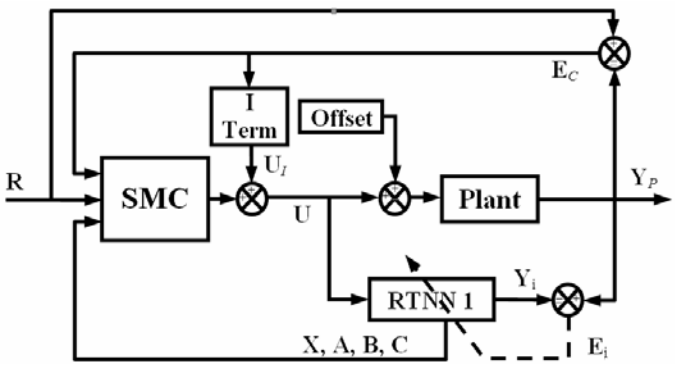

Figure 3. Block diagram of the indirect adaptive SM control with I-term

It contained a recurrent neural identifier RTNN 1, and a Sliding Mode (SM) controller with entries – the reference signal R, the output error Ec, and the states X and parameters A, B, C, estimated by the neural identifier RTNN-1. The total control is a sum of the SM control and the I-term control, computed using the equation

(26) V(k+1) = V(k) + To Ec(k).

The linearization of the activation functions of the local learned identification RTNN-1 model, which approximated the plant, leads to the following linear local plant model:

(27) X(k+1) = AX(k) + BU(k); Y(k) = CX(k).

Where L > M (rectangular system), is supposed. Let us define the following sliding surface with respect to the output tracking error

(28) $$S(k+1) = E(k+1) + \sum_{i=1}^{P} \gamma_i E(k-i+1);\ |\gamma_i| < 1,$$

where S(.) is the sliding surface error function; E(.) is the systems local output tracking error; γ_i are parameters of the local desired error function; P is the order of the error function. The additional inequality in (28) is a stability condition, required for the sliding surface error function. The local tracking error is defined as E(k) = R(k) – Y(k), where R(k) is a L-dimensional local reference vector and Y(k) is an local output vector with the same dimension. The objective of the sliding mode control systems design is to find a control action which maintains the systems error on the sliding surface assuring that the output tracking error reached zero in P steps, where P<N, which is fulfilled if S(k+1) = 0. As the local approximation plant model (27) is controllable, observable and stable, [10], [15], the matrix A is block-diagonal, and L>M (rectangular system is supposed), the matrix product (CB) is nonsingular with rank M, and the plant states X(k) are smooth non- increasing functions. Now, from (27), (28) it is easy to obtain the equivalent control capable to lead the system to the sliding surface which yields:

(29) $$U_{eq}(k) = (CB)^+ \left[-CAX(k) + R(k+1) + \sum_{i=1}^{P} \gamma_i E(k-i+1) \right];$$

(30) $$(CB)^+ = [(CB)^T (CB)]^{-1} (CB)^T.$$

The SMC avoiding chattering is taken using a saturation function inside a bounded control level taking into account plant uncertainties. The proposed SMC cope with the characteristics of the wide class of plant model reduction neural control with reference model, and represents an indirect adaptive neural control.

Optimal control with I-term. The block-diagram of the optimal control system is given on *figure 4*.

It contained a recurrent neural identifier RTNN 1, and an optimal controller with entries – the reference signal R, the output of the I-term block V, (26), and the states X and parameters A, B, C, estimated by the neural identifier RTNN-1. The optimal control algorithm with I-term could be obtained extending the linearized model (27) with the model of the I-term (26). The state space equation of the extended system is given by the following equation:

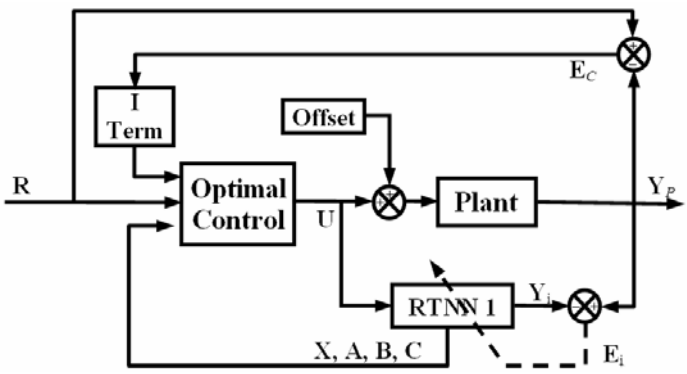

Figure 4. Block diagram of the real-time optimal control with I-term containing RTNN identifier and optimal controller

(31) $X_e(k+1) = A_e X_e(k) + B_e U(k)$,

where $X_e = [X|V]^T$ is a state vector with dimension (L+N) and

$$A_e = \begin{bmatrix} A & 0 \\ -(CB)^+ CA & I \end{bmatrix}; B_e = \begin{bmatrix} B \\ -I \end{bmatrix}.$$

The optimal I-term control is given by

(32) $U(k) = -[B_e^T P_e(k) B_e + R]^{-1}[B_e^T P_e(k) B_e] X_e(k)$,

where the P_e is solution of the discrete Riccati equation

$$P_e(k+1)=A_e^T[P_e(k)-P_e(k)B_e(B_e^T P_e(k)B_e+R)^{-1}B_e^T P_e(k)]A_e+Q.$$

The given up optimal control is rather complicated and here it is used only for purpose of comparison.

4. Analytical Model of the Distributed Parameter Bioprocess Plant

The block diagram of the anaerobic digestion systems is depicted on *figure 5*.

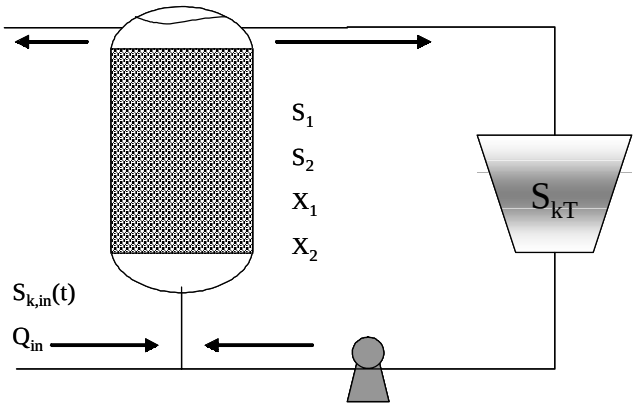

Figure 5. Block-diagram of the anaerobic digestion bioreactor

It consists of a fixed bed bioreactor, pump and a recirculation tank. The physical meaning of all variables and constants (also its values), are summarized on *table 1*.

The PDE anaerobic digestion bioprocess model, [14], is described by the following equations:

(33) $$\frac{\partial X_1}{\partial t} = (\mu_1 - \varepsilon D) X_1, \quad \mu_1 = \mu_{1\max} \frac{S_1}{K'_{s_1} X_1 + S_1},$$

(34) $$\frac{\partial X_2}{\partial t} = (\mu_2 - \varepsilon D) X_2, \quad \mu_2 = \mu_{2s} \frac{S_2}{K'_{s_2} X_2 + S_2 + \frac{S_2^2}{K_{I_2}}},$$

(35) $$\frac{\partial S_1}{\partial t} = \frac{E_z}{H^2}\frac{\partial^2 S_1}{\partial z^2} - D\frac{\partial S_1}{\partial t} - k_1 \mu_1 X_1,$$

(36) $$\frac{\partial S_2}{\partial t} = \frac{E_z}{H^2}\frac{\partial^2 S_2}{\partial z^2} - D\frac{\partial S_2}{\partial t} + k_2 \mu_1 X_1,$$

(37) $$S_1(0,t) = \frac{S_{1,in}(t) + RS_{1T}}{R+1}, \quad S_2(0,t) = \frac{S_{2,in}(t) + RS_{2T}}{R+1}, \quad R = \frac{Q_T}{DV_{eff}},$$

(38) $$\frac{\partial S_1}{\partial z}(1,t) = 0, \quad \frac{\partial S_2}{\partial z}(1,t) = 0.$$

(39) $$\frac{dS_{1T}}{dt} = \frac{Q_T}{V_T}(S_1(1,t) - S_{1T}), \quad \frac{dS_{2T}}{dt} = \frac{Q_T}{V_T}(S_2(1,t) - S_{2T}).$$

For practical purpose, the full PDE anaerobic digestion process model could be reduced to an ODE system using an early lumping technique and the Orthogonal Collocation Method (OCM), [6], [15]. The precision of the OCM approximation of the PDE model depended on the number of measurement (collocation) points, but the approximation is always exact in that points. If the number of points is very high and the point positions are chosen inappropriately, the ODE model could loose identifiability. Furthermore the ODE plant model here is used as a plant data generator for neural identification and control of PDE system and the number of point not need to be too high. So to fulfill this objective we need a reduced order model having only four points, (0.2H, 0.4 H, 0.6H, 0.8H), but generating 18 measured variables ($X_{1,i}$; $X_{2,i}$; $S_{1,i}$; $S_{2,i}$; i=1-4 plus S_{1T}, S_{2T} for the recirculation tank). So the plant input/output dimensions are M=2, L=18. The reference set points generated for all that variables keep the form but differ in amplification due to its position. The plant ODE system model, obtained by OCM is

(40) $$\frac{dX_{1,i}}{dt} = (\mu_{1,i} - \varepsilon D) X_{1,i}, \quad \frac{dX_{2,i}}{dt} = (\mu_{2,i} - \varepsilon D) X_{2,i},$$

(41) $$\frac{dS_{1,i}}{dx} = \frac{E_z}{H^2}\sum_{j=1}^{N+2} B_{i,j} S_{1,j} - D\sum_{j=1}^{N+2} A_{i,j} S_{1,j} - k_1 \mu_{1,i} X_{1,i},$$

(42) $$\frac{dS_{1T}}{dt} = \frac{Q_T}{V_T}(S_1(1,t) - S_{1T}), \quad \frac{dS_{2T}}{dt} = \frac{Q_T}{V_T}(S_2(1,t) - S_{2T}).$$

(43) $$\frac{dS_{2,i}}{dt} = \frac{E_z}{H^2}\sum_{j=1}^{N+2} B_{i,j} S_{1,j} - D\sum_{j=1}^{N+2} A_{i,j} S_{2,j} + k_2 \mu_{1,i} X_{2,i} - k_3 \mu_{2,i} X_{2,i},$$

(44) $$\frac{dS_{1T}}{dt} = \frac{Q_T}{V_T}(S_{1,N+2} - S_{1T}), \quad \frac{dS_{2T}}{dt} = \frac{Q_T}{V_T}(S_{2,N+2} - S_{2T}),$$

(45) $$S_{k,1} = \frac{1}{R+1} S_{k,in}(t) + \frac{R}{R+1} S_{kT},$$

(46) $$S_{k,N+2} = \frac{K_1}{R+1} S_{k,in}(t) + \frac{K_1 R}{R+1} S_{kT} + \sum_{i=2}^{N+1} K_i S_{k,i}$$

Table 1. Summary of the variables in the plant model

Variable	Units	Name	Value
Z	$z \in [0,1]$	*Space variable*	
T	D	*Time variable*	
E_z	M^2/d	*Axial dispersion coefficient*	1
D	1/d	*Dilution rate*	0.55
H	M	*Fixed bed length*	3.5
X_1	g/L	*Concentration of acidogenic bacteria*	
X_2	g/L	*Concentration of methanogenic bacteria*	
S_1	g/L	*Chemical Oxygen Demand*	
S_2	Mmol/L	*Volatile Fatty Acids*	
ε		*Bacteria fraction in the liquid phase*	0.5
k_1	g/g	*Yield coefficients*	42.14
k_2	g/g	*Yield coefficients*	250
k_3	g/g	*Yield coefficients*	134
μ_1	1/d	*Acidogenesis growth rate*	
μ_2	1/d	*Methanogenesis growth rate*	
μ_{1max}	1/d	*Kinetic parameter*	1.2
$\mu_{2s,}$	1/d	*Kinetic parameter*	0.74
$K_{1s,}$	g/g	*Kinetic parameter*	50.5
$K_{2s,}$	g/g	*Kinetic parameter*	16.6
K_{I2}	g/g	*Kinetic parameter*	256
Q_T	M^3/d	*Recycle flow rate*	0.24
V_T	M^3	*Volume of the recirculation tank*	0.2
S_{1T}	g/L	*Concentration of Chemical Oxygen Demand in the recirculation tank*	
S_{2T}	Mmol/L	*Concentration of Volatile Fatty Acids in the recirculation tank*	
Q_{in}	M^3/d	*Inlet flow rate*	0.31
V_B	M^3	*Volume of the fixed bed*	1
V_{eff}	M^3	*Effective volume tank*	0.95
$S_{1,in}$	g/l	*Inlet substrate concentration*	
$S_{2,in}$	Mmol/L	*Inlet substrate concentration*	

(47) $$K_1 = -\frac{A_{N+2,1}}{A_{N+2,N+2}}, \quad K_i = -\frac{A_{N+2,i}}{A_{N+2,N+2}},$$

(48) $$A = \Lambda\phi^{-1}, \quad \Lambda = \left[\varpi_{m,l}\right], \quad \varpi_{m,l} = (l-1)z_m^{l-2},$$

(49) $$B = \Gamma\phi^{-1}, \quad \Gamma = \left[\tau_{m,l}\right], \quad \tau_{m,l} = (l-1)(l-2)z_m^{l-3}, \phi_{m,l} = z_m^{l-1}$$

(50) $$i = 2,...,N+2, \quad m,l = 1,...,N+2.$$

The described above simplified model will be used as data generator for system identification and control simulations.

5. Graphical Simulation Results

Simulation results of system identification. The centralized RTNN identified 18 output plant variables, which are 4 variables for each collocation point z=0.2H, z=0.4H, z=0.6H, z=0.8H of the fixed bed as: X_1 (acidogenic bacteria), X_2 (methanogenic bacteria), S_1 (chemical oxygen demand) and S_2 (volatile fatty acids), and the next variables in the recirculation tank: S_{1T} (chemical oxygen demand) and S_{2T} (volatile fatty acids). The two plant inputs are S_{1in} (concentration of acidogenic bacteria in the substrate) and S_{2in} (concentration of methanogenic bacteria in the substrate). For lack of space we shall show graphical results only for the X_2 variable. The topology of the RTNN-1 is (2, 20, 18), the activation functions are tanh(.) for both layers. The learning rate parameters for the BP algorithm of learning are α=0, η=0.4, and for the L-M learning – the forgetting factor is α=1, the regularization constant is ρ=0.001, and the initial value of the P matrix is an identity matrix with dimension 420x420. The simulation results of RTNN-1 system identification are obtained on-line during 400 days with a step of 0.5 day. The identification inputs used are

$$S_{1in} = 0.5 + 0.02\sin\left(\frac{\pi t}{100}\right) + 0.1\sin\left(\frac{3\pi t}{100}\right) + 0.04\cos\left(\frac{\pi t}{100}\right),$$
$$S_{2in} = 0.5 + 0.1\sin\left(\frac{\pi t}{100}\right) + 0.1\sin\left(\frac{5\pi t}{100}\right) + 0.1\cos\left(\frac{8\pi t}{100}\right).$$

Table 2 and *table 3* compared the Means Squared Error (MSE%) results of the BP and L-M neural identification of plant

Table 2. MSE% of the BP identification of all output plant variables in all measurement points

Colloc. point	X_1	X_2	S_1 / S_{1T}	S_2 / S_{2T}
z=0.2	5.9981E-7	2.1006E-6	1.5901E-4	2.8282E-4
z=0.4	3.7111E-7	1.6192E-6	9.8240E-5	2.0506E-4
z=0.6	2.3145E-7	1.1308E-6	6.1119E-5	1.3908E-4
z=0.8	1.4997E-7	7.7771E-7	3.9595E-5	9.4061E-5
Recirc Tank	-	-	3.0694E-5	7.3404E-5

Table 3. MSE% of the L-M identification of all output plant variables in all measurement points

Colloc. point	X_1	X_2	S_1 / S_{1T}	S_2 / S_{2T}
z=0.2	5.0843E-7	1.8141E-6	1.3510E-4	2.5476E-4
z=0.4	3.1428E-7	1.3934E-6	8.3839E-5	1.8217E-4
z=0.6	1.961E-7	9.6976 E-7	5.2303E-5	1.2200E-4
z=0.8	1.2669E-7	6.6515E-7	3.3940E-5	8.1905E-5
Recirc Tank	–	–	2.6318E-5	6.3791E-5

variables for the fixed bed and the recirculation tank.

The *figures 6-8* showed the BP identification of the variable X_2 in four collocation points. The *figures 9-11* showed the L-M identification of the same variable X_2 in the same four collocation points.

Note that the form of the plant process variables in the different measurement points is equal but the amplitude is different depending on the point position. The given in *table 2* and *table 3* MSE results showed slight priority of the L-M learning algorithm over the BP one. The comparison of *figure 7* and *figure 10* showed that the L-M algorithm converged faster than the BP algorithm but it is paid with a greater complexity of the L-M one.

Simulation results of the centralized sliding mode adaptive control with I-term. In this case the indirect adaptive I-term control is a sum of the I-term control signal and the SM control

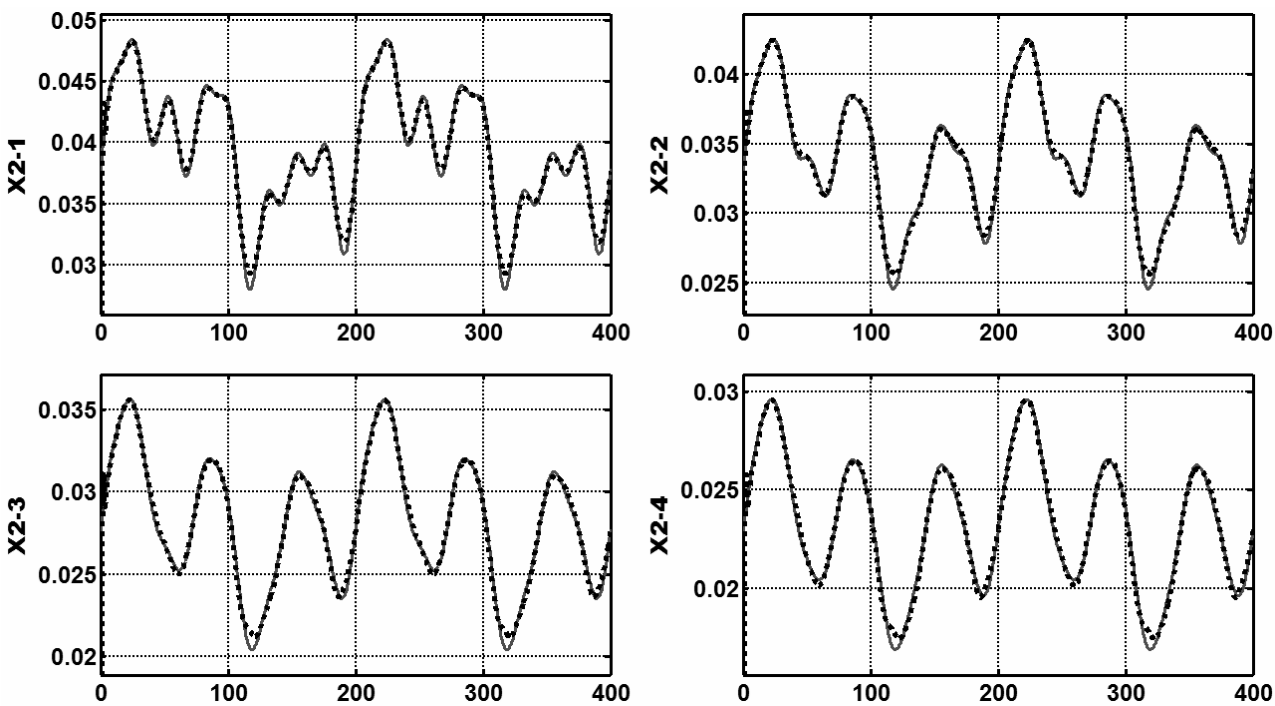

Figure 6. Neural identification of the plant output X_2 in four measurement points for the total time of BP learning : a) z=0.2H, b) z=0.4H, c) z=0.6H, d) z=0.8H

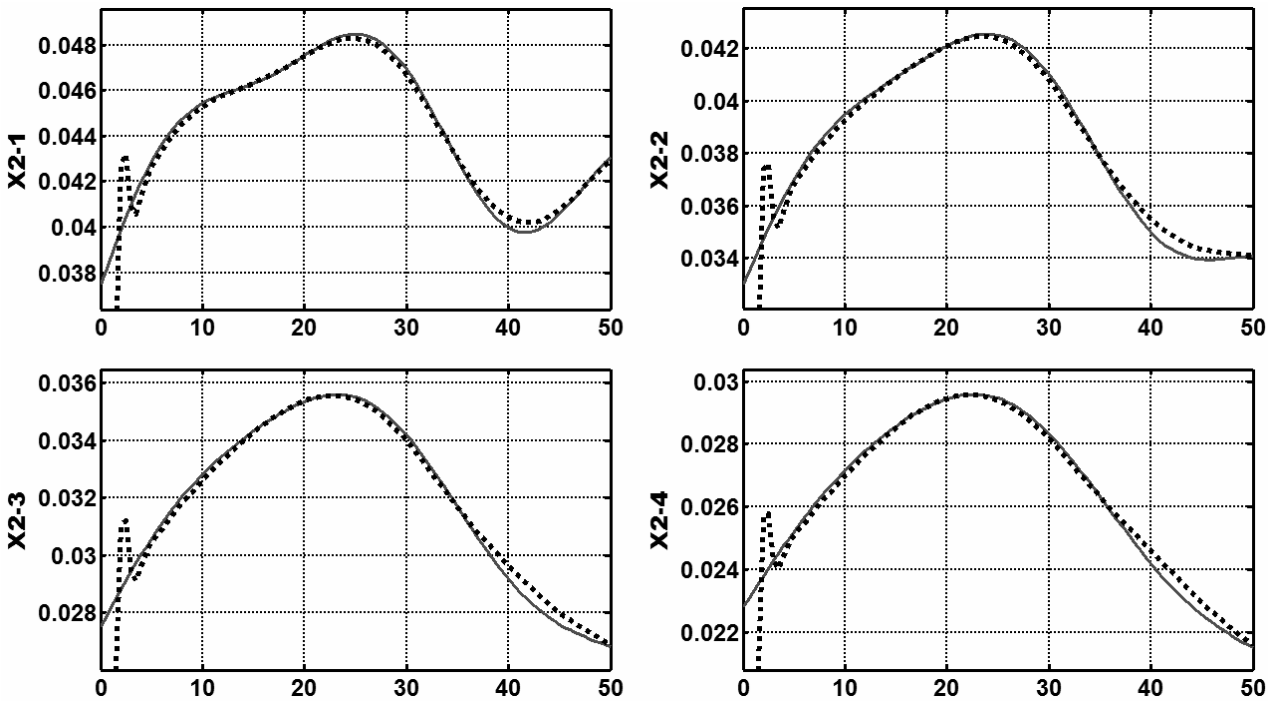

Figure 7. Neural identification of the plant output X_2 in four measurement points for the beginning of BP learning: a) z=0.2H, b) z=0.4H, c) z=0.6H, d) z=0.8H

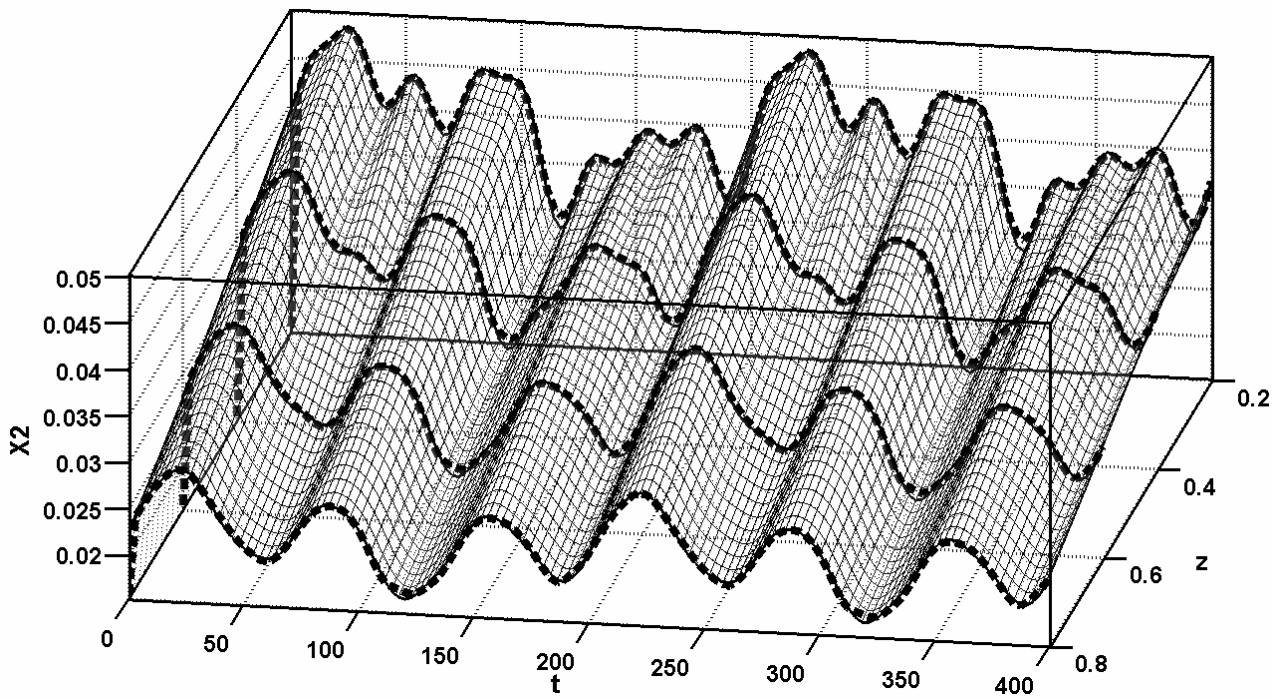

Figure 8. Three dimensional plot of the neural identification of the plant output X_2 in four measurement points of BP learning: a) z=0.2H, b) z=0.4H, c) z=0.6H, d) z=0.8H

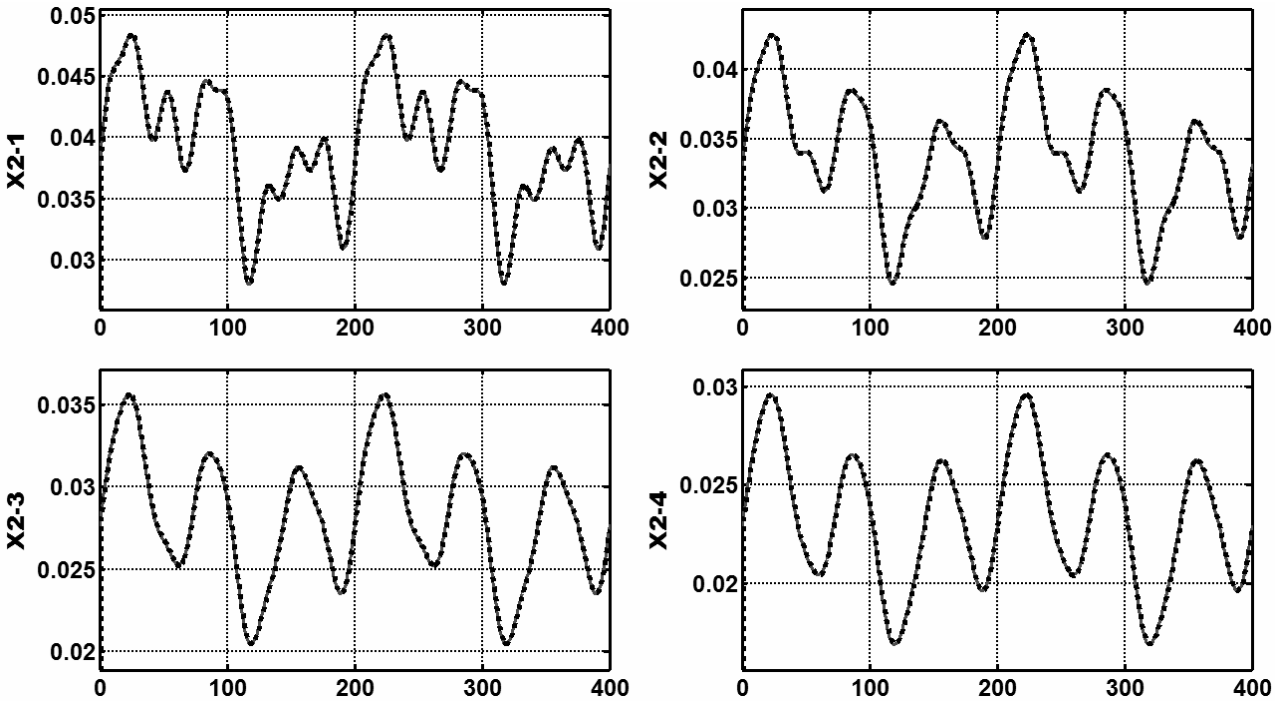

Figure 9. Neural identification of the plant output X_2 in four measurement points for the total time of L-M learning: a) z=0.2H, b) z=0.4H, c) z=0.6H, d) z=0.8H

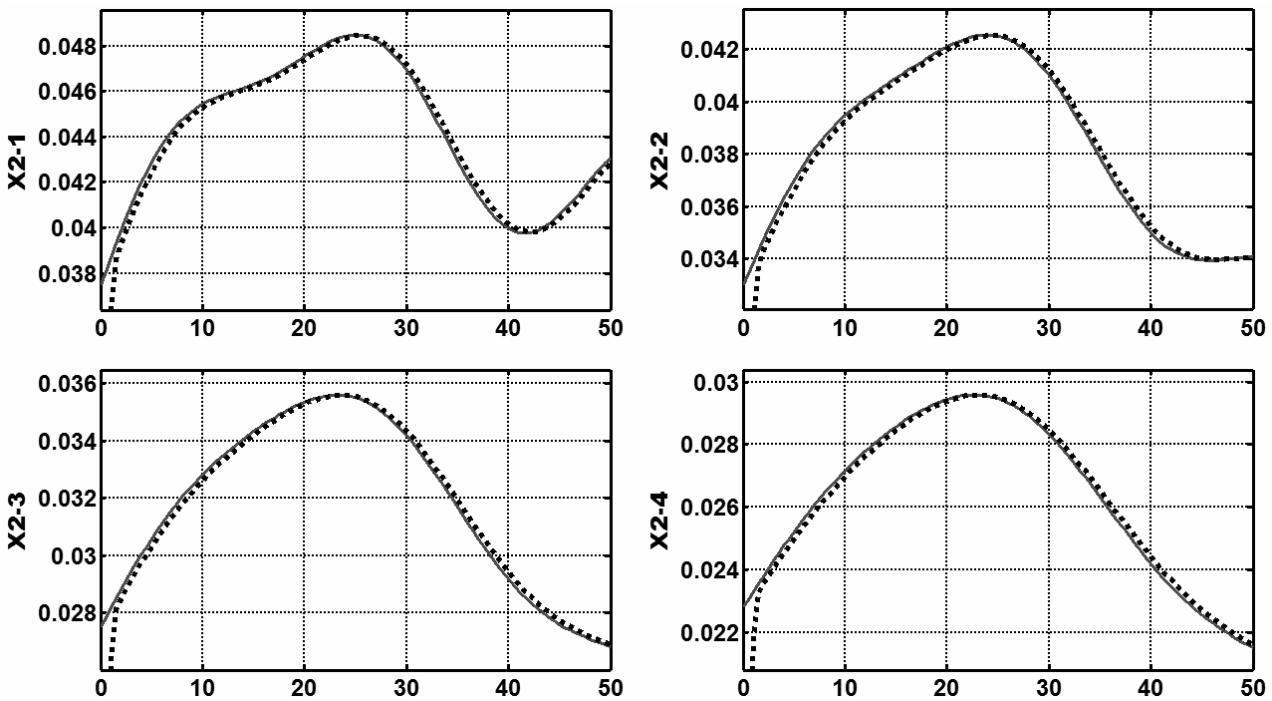

Figure 10. Neural identification of the plant output X_2 in four measurement points for the beginning of L-M learning: a) z=0.2H, b) z=0.4H, c) z=0.6H, d) z=0.8H

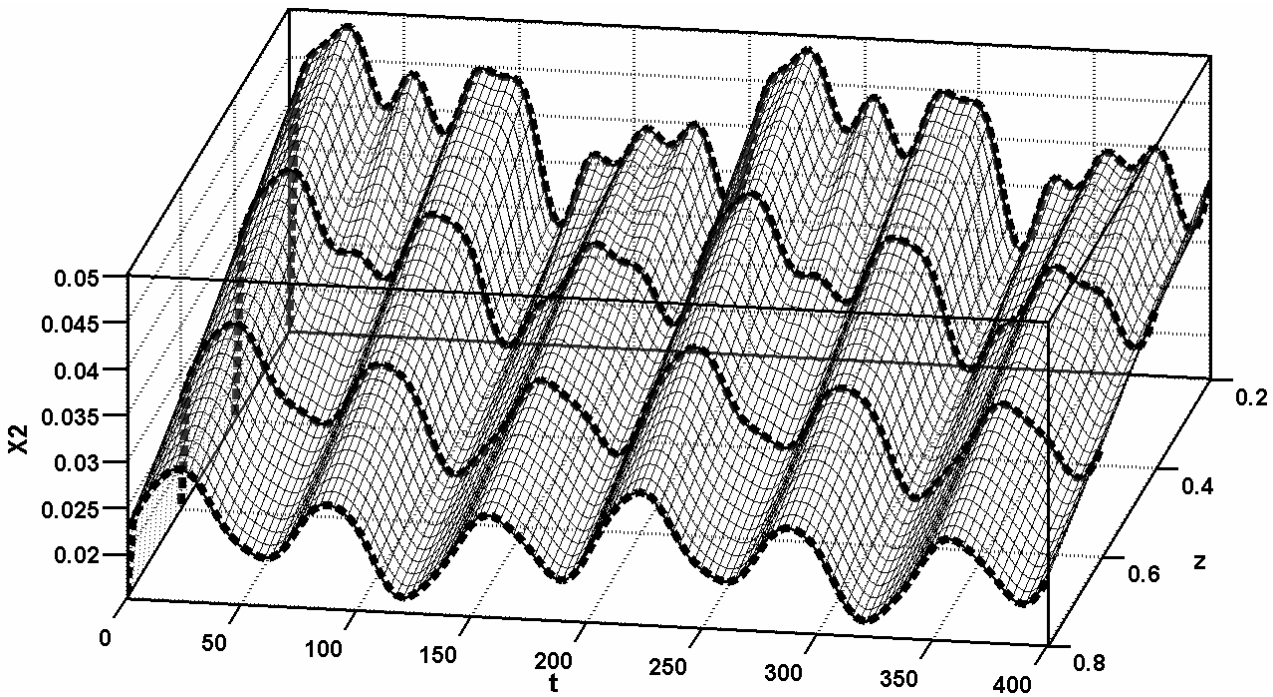

Figure 11. Three dimensional plot of the neural identification of the plant output X_2 in four measurement points of L-M learning: a) z=0.2H, b) z=0.4H, c) z=0.6H, d) z=0.8H

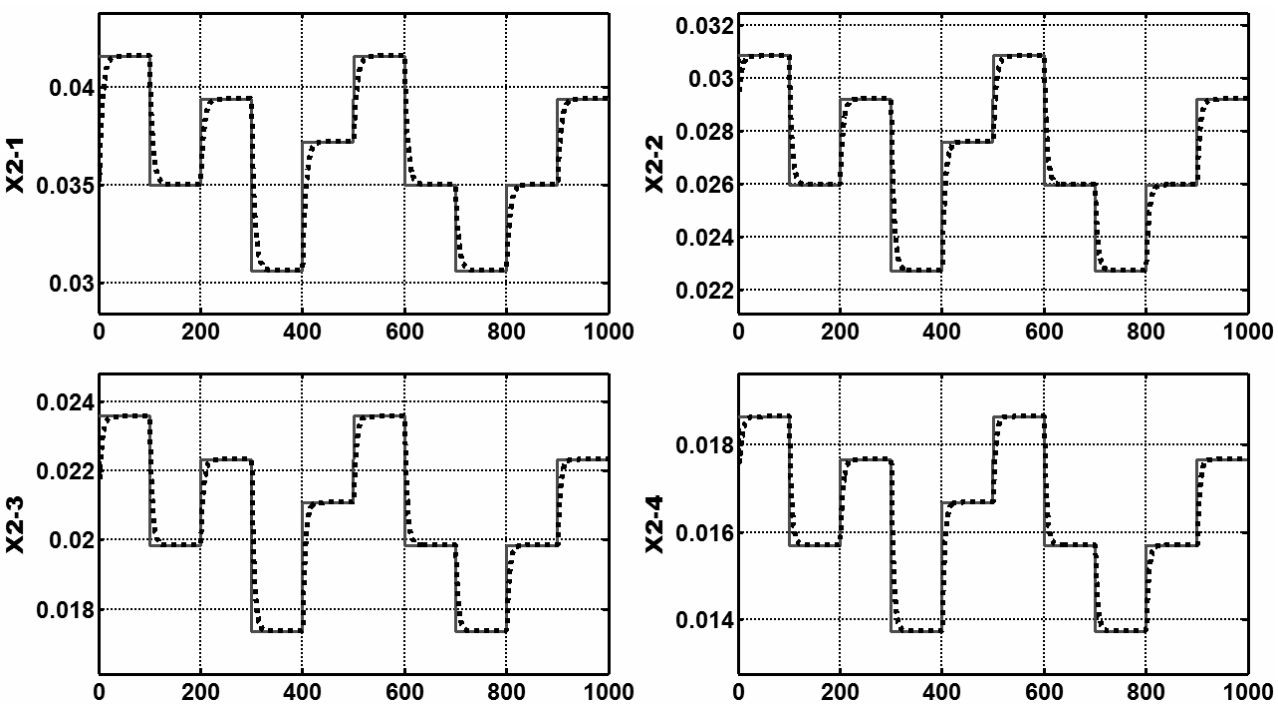

Figure 12. I-term indirect control of the plant output X_2 in four measurement points for the total time of L-M learning: a) z=0.2H, b) z=0.4H, c) z=0.6H, d) z=0.8H

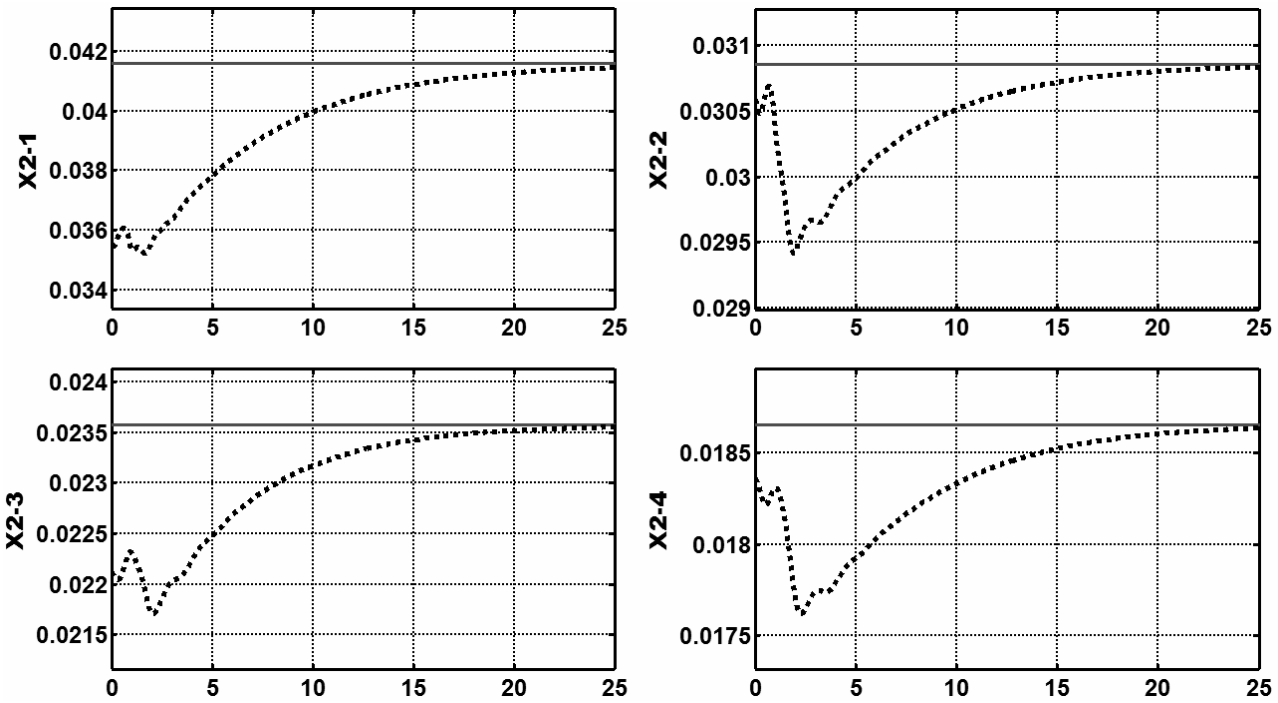

Figure 13. I-term indirect SM control of the plant output X_2 in four measurement points for the beginning of L-M learning: a) z=0.2H, b) z=0.4H, c) z=0.6H, d) z=0.8H

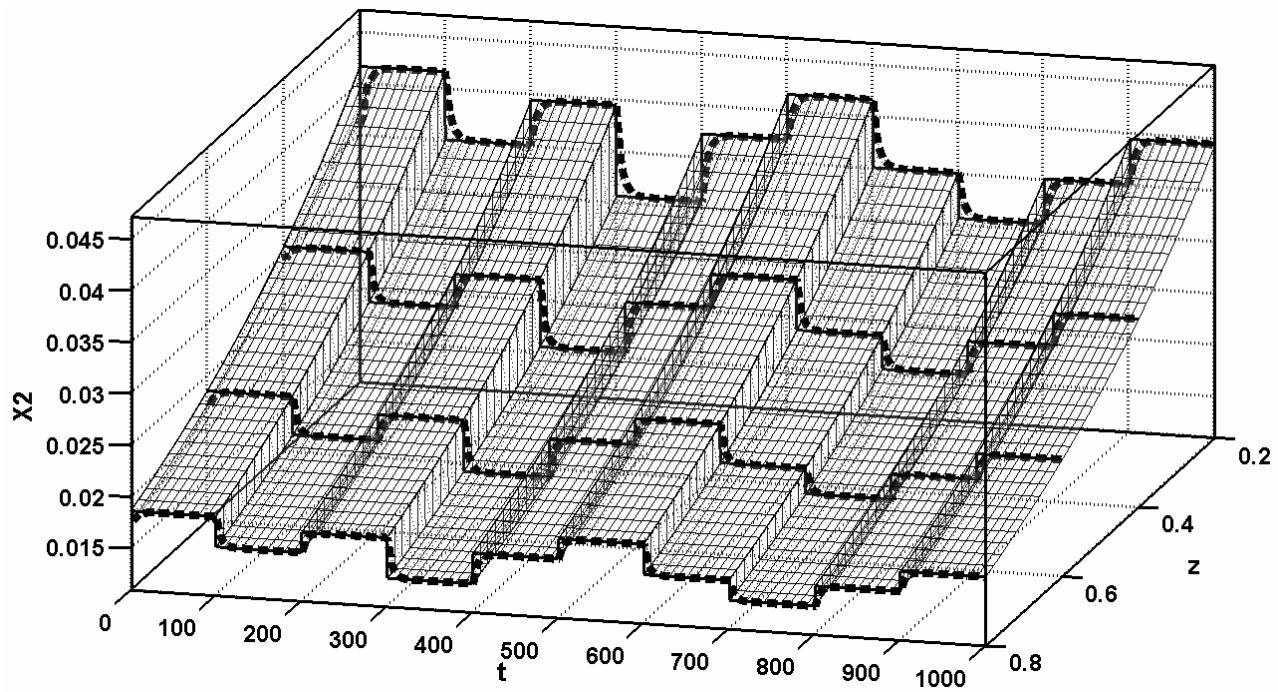

Figure 14. Three dimensional plot of the I-term indirect SM control of the plant output X_2 in four measurement points of L-M learning: a) z=0.2H, b) z=0.4H, c) z=0.6H, d) z=0.8H

Table 4. MSE% of the I-term indirect SMC of all output plant variables in all measurement points

Colloc. point	X_1	X_2	S_1 / S_{1T}	S_2 / S_{2T}
z=0.2	2.6969E-8	1.7122E-7	9.9526E-6	2.1347E-5
z=0.4	1.3226E-8	1.2511E-7	5.2323E-6	1.2903E-5
z=0.6	1.0873E-8	6.5339E-8	3.2234E-6	7.0511E-6
z=0.8	5.9589E-9	4.4750E-8	1.6759E-6	4.4548E-6
Recirc Tank	-	-	1.1842E-6	2.5147E-6

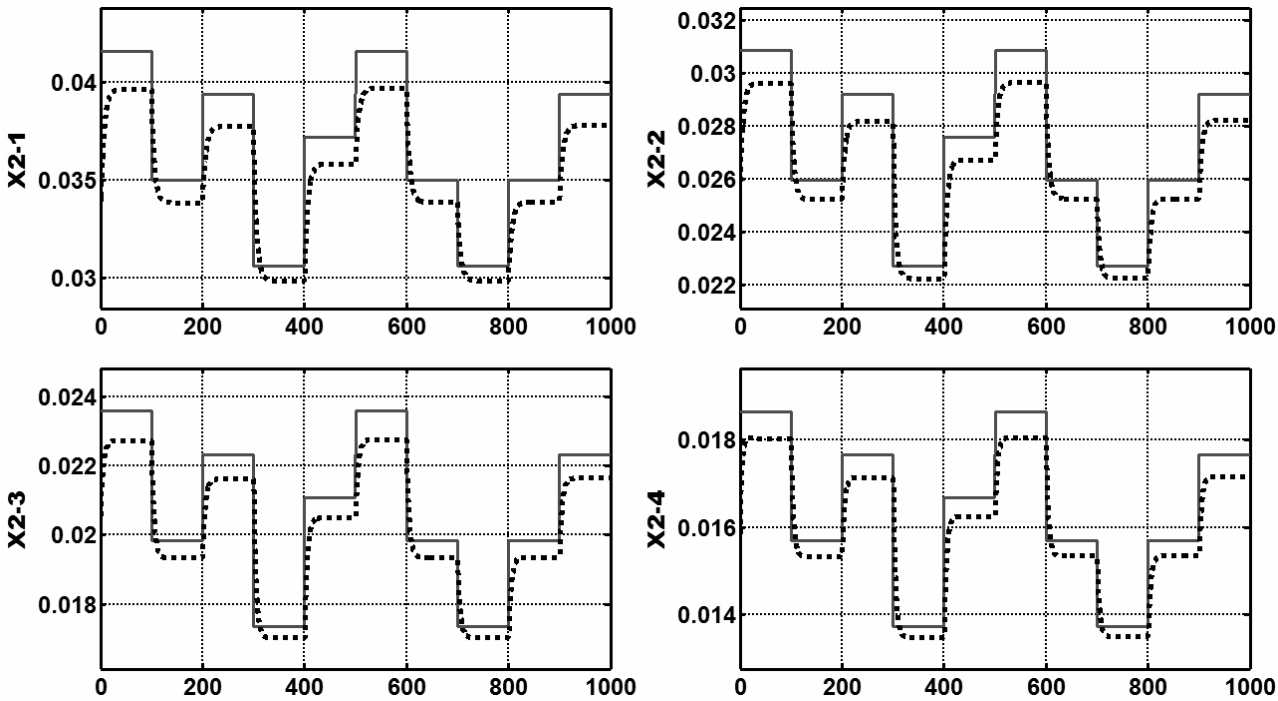

Figure 15. Indirect control without I-term of the plant output X_2 in four measurement points for the total time of L-M learning: a) z=0.2H, b) z=0.4H, c) z=0.6H, d) z=0.8H

computed using the state and parameter information issued from the RTNN-1 neural identifier. The X_2 control simulation results are given on *figures 12-14*.

The MSE numerical results for all final process variable and measurement points, given on *table 4*, possessed small values.

The given on *figures 12-14* graphical results of I-term SMC showed smooth exponential behavior, fast convergence and the removal of the constant noise terms and uncertainties. *Figure 15* illustrated the behavior of the SMC system without I-term perturbed by a constant noise. It showed that the constant input perturbation of the plant caused a deviation of the plant output X_2 with respect of the set point R_2 and this occurred for all other plant output signals and measurement points.

Simulation results of the centralized I-term optimal control using neural identifier and L-M learning. The integral term extended the identified local linear plant model so it is part of the indirect optimal control algorithm. *Figures 16-18* illustrated the X_2 I-term optimal control results. The MSE numerical results for all final process variable and measurement points control results, given on *table 5* possessed small values.

The given on *figures 16-18* graphical results of I-term optimal control showed smooth exponential behaviour, fast convergence and the removal of the constant noise terms.

Conclusions

The paper proposes a new neural identification and control methodology for distributed parameter bioprocess plant. The simplification of the DPS given by PDEs is realized using the orthogonal collocation method in three collocation points, converting the PDE plant description in ODE one. The system is identified using RTNN model and BP and L-M learning, where a high precision of convergence is achieved (the final MSE% for both BP and L-M learning algorithms is of order of E-4). The comparative results showed a slight priority in precision and convergence of the L-M over the BP. The obtained simulation results of centralized adaptive indirect SM and optimal control with I-term exhibited a good convergence and precise reference tracking. The MSE% of plant outputs tracking for the two considered methods of control is of order of E-5 in the worse case.

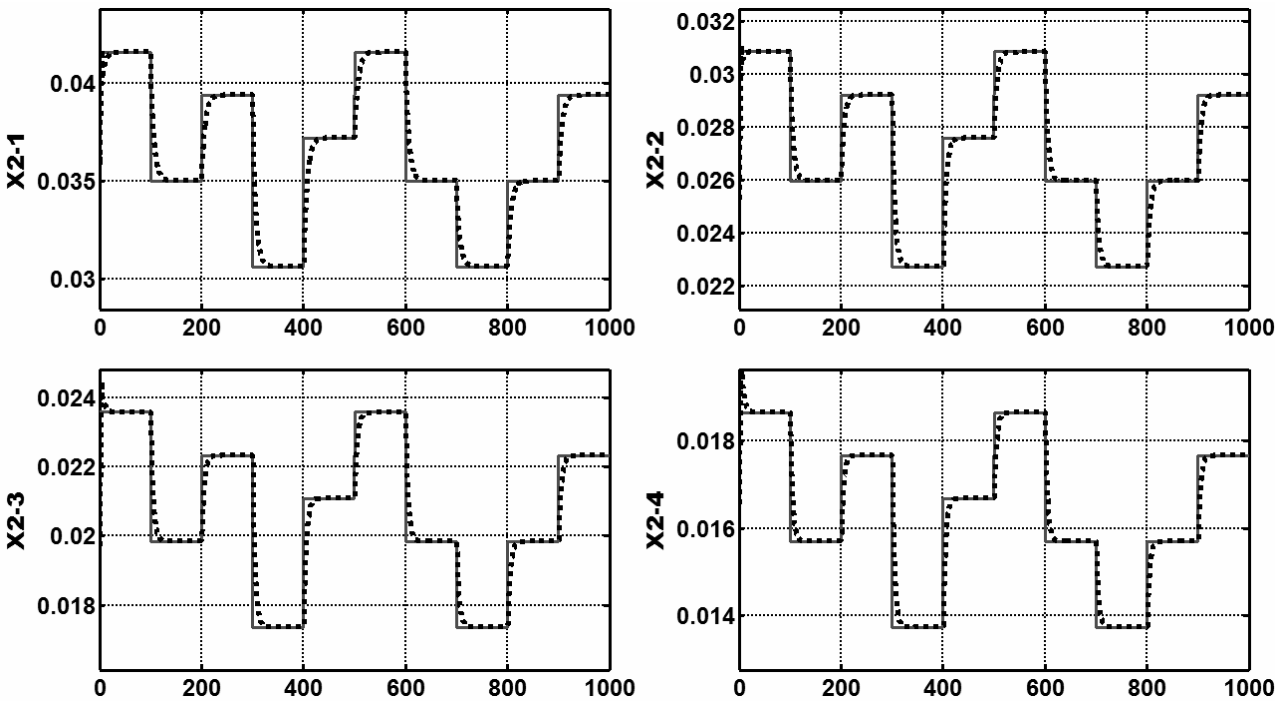

Figure 16. I-term optimal control of the plant output X_2 in four measurement points for the total time of L-M learning: a) z=0.2H, b) z=0.4H, c) z=0.6H, d) z=0.8H

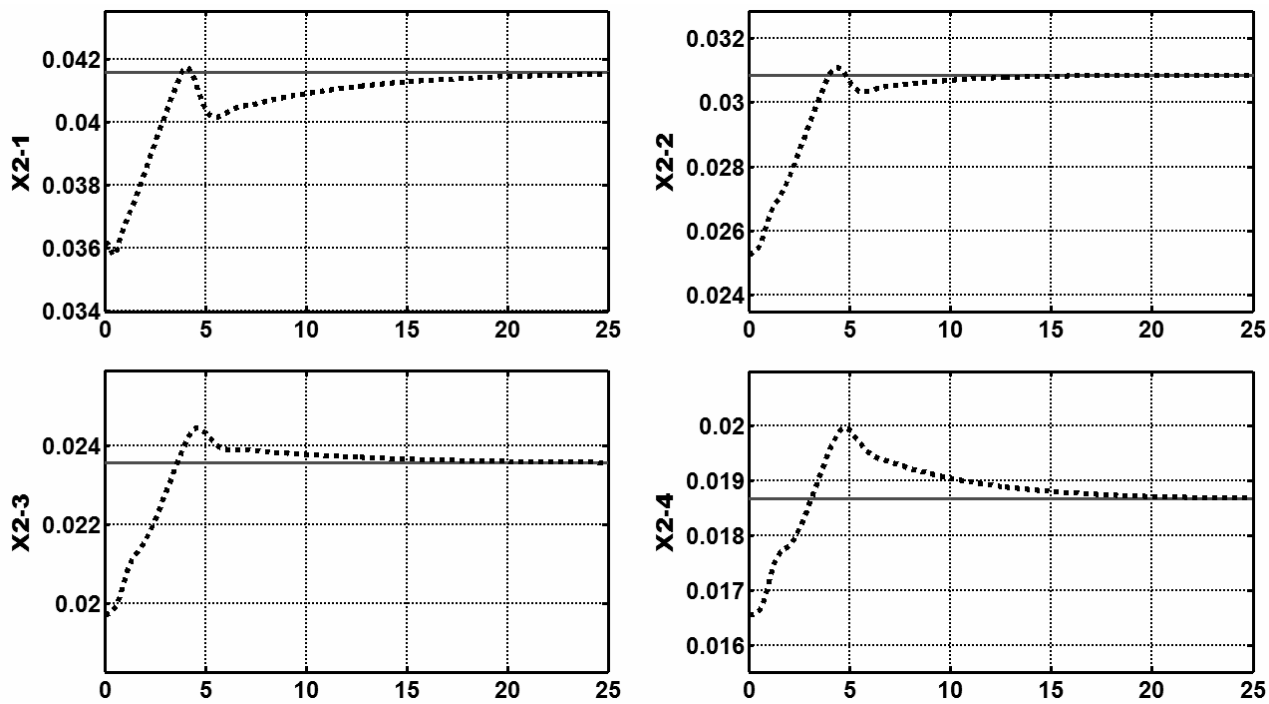

Figure 17. I-term optimal control of the plant output X_2 in four measurement points for the beginning of L-M learning: a) z=0.2H, b) z=0.4H, c) z=0.6H, d) z=0.8H

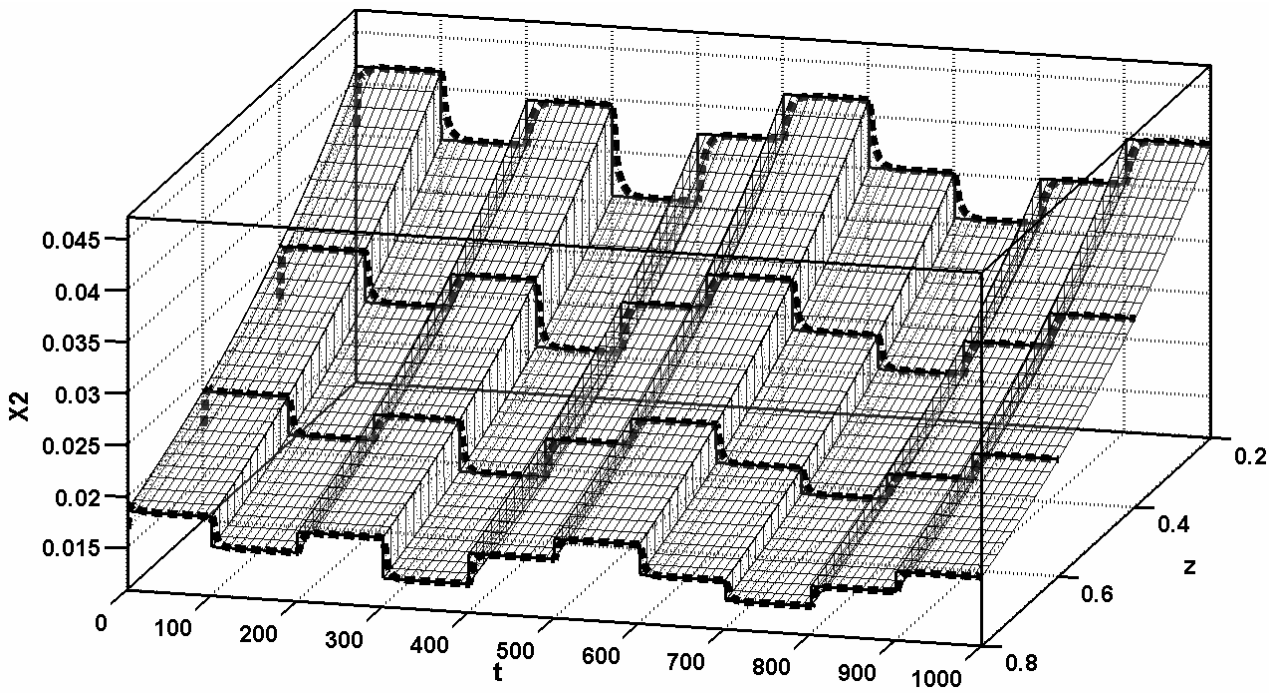

Figure 18. Three dimensional plot of the I-term optimal control of the plant output X_2 in four measurement points of L-M learning: a) z=0.2H, b) z=0.4H, c) z=0.6H, d) z=0.8H

Table 5. MSE% of the I-term optimal control of all output plant variables in all measurement points

Colloc. point	X_1	X_2	S_1 / S_{1T}	S_2 / S_{2T}
z=0.2	2.0672E-8	1.5262E-7	9.3626E-6	1.4949E-5
z=0.4	1.3819E-8	7.5575E-8	5.6917E-6	1.0197E-5
z=0.6	1.8115E-8	4.7505E-8	2.8872E-6	6.1763E-6
z=0.8	1.5273E-8	5.9744E-8	1.6295E-6	4.2868E-6
Recirc Tank	-	-	1.3042E-6	2.5136E-6

The graphical simulation results showed that all control methods with I-term could compensate constant plant input noises and the I-term removal caused a system outputs deviation from the reference signals. The MSE study ordered the control methods used as: indirect optimal and sliding mode, but the difference between them is little.

Acknoweledgements

The Ph.D. student Eloy Echeverria Saldierna is thankful to CONACYT, Mexico for the scholarship received during his studies at the Department of Automatic Control, CINVESTAV-IPN, Mexico.

References

1. Haykin, S. Neural Networks, a Comprehensive Foundation. Second Edition. Section 2.13, p.84-89; Section 4.13, 208-213. Prentice-Hall, Upper Saddle River New Jersey 07458, 1999.

2. Bulsari, A., S. Palosaari. Application of Neural Networks for System Identification of an Adsorption Column. – *Neural Computing and Applications*, 1, 1993, 160-165.

3. Deng, H., H. X. Li. Hybrid Intelligence Based Modelling for Nonlinear Distributed Parameter Process with Applications to the Curing Process. – *IEEE Transactions on Systems, Man and Cybernetics*, 4, 2003, 3506-3511.

4. Deng, H., H.X. Li. Spectral – Approximation – Based Intelligent Modelling for Distributed Thermal Processes. IEEE Transactions on Control Systems Technology, 13, 2005, 686-700.

5. Gonzalez-Garcia, R., R. Rico-Martinez, I. Kevrekidis. Identification of Distributed Parameter Systems: A Neural Net Based Approach. – *Computers, and Chemical Engineering*, 22, 1998, No 4-supl. 1, 965-968.

6. Aguilar-Garnica, E., V. Alcaraz-Gonzalez, V. Gonzalez-Alvarez. Interval Observer Design for an Anaerobic Digestion Process Described by a Distributed Parameter Model. Proceedings of the 2-nd Int. Meeting on Environmental Biotechnology and Engineering (2IMEBE), 26-29 Sept. 2006, Mexico City, Mexico, 2006, paper 117, 1-16.

7. Padhi, R., S. Balakrishnan, T. Randolph. Adaptive Critic Based Optimal Neurocontrol Synthesis for Distributed Parameter Systems. – *Automatica*, 37, 2001, 1223-1234.

8. Padhi, R., S. Balakrishnan. Proper Orthogonal Decom-position Based Optimal Neurocontrol Synthesis of a Chemical Reactor Process Using Approximate Dynamic Programming. – *Neural Networks,* 16, 2003, 719-728.

9. Pietil, S., H. N. Koivo. Centralized and Decentralized Neural Network Models for Distributed Parameter Systems. Proceedings of the Sympo-

sium on Control, Optimization and Supervision, CESA'96. IMACS Multiconference on Computational Engineering in Systems Applications, Lille, France, 1996, 1043-1048.

10. Baruch, I. S., P. Georgieva, J. Barrera-Cortes, S. Feyo de Azevedo. Adaptive Recurrent Neural Network Control of Biological Wastewater Treatment. International Journal of Intelligent Systems (Special Issue on Soft Computing for Modeling, Simulation and Control of Nonlinear Dynamical Systems, O. Castillo, and P. Melin, Guest Eds.). WILEY Inter-Science, ISSN 0884-8173, 20, 2005, No. 2, 173-194.

11. Baruch, I. S., C. R. Mariaca-Gaspar, J. Barrera-Cortes. Recurrent Neural Network Identification and Adaptive Neural Control of Hydrocarbon Biodegradation Processes. Xiaolin Hu and P. Balasubramaniam, Eds. Recurrent Neural Networks, ISBN 978-953-7619-08-4, Croatia. I-Tech/ ARS Press, 2008, Ch. 4,.61-88.

12. Baruch, I. S., J. Barrera-Cortes, L .A. Hernandez. A Fed-Batch Fermentation Process Identification and Direct Adaptive Neural Control with Integral Term. Proceedings of MICAI 2004: Advances in Artificial Intelligence, LNAI 2972, R. Monroy, G. Arroyo-Figueroa, L. E. Sucar, and H. Sossa, Eds., ISBN 3-540-21459-3, Berlin Heidelberg New York, Springer-Verlag, 2004, 764-773.

13. Baruch, I. S., J. M. Flores, F. Nava, I. R. Ramirez, B. Nenkova. An Advanced Neural Network Topology and Learning, Applied for Identification and Control of a D.C. Motor. Proceedings of the 1st Int. IEEE Symposium on Intelligent Systems, IS'02, Varna, Bulgaria, 1, 2002, 289-295.

14. Baruch, I. S., L. A. Hernandez, J. Barrera-Cortes. Recurrent Neural Identification and Sliding Mode Adaptive Control of an Aerobic Fermentation Plant. Cientifica, ESIME-IPN, ISSN 1665-0654, 11, 2007, No. 2, 55-62.

15. Baruch, I. S., R. Galvan-Guerra, B. Nenkova. Centralized Recurrent Neural Identification and Control of an Anaerobic Digestion Bioprocess. Proc. International Conference Automatics and Informatics, Sofia, Bulgaria, Oct. 1-4, 2008, ISSN 1313-1850, Section XI, Intelligent Systems, UAI, SAI, 2008, XI-1 to XI-4.

16. Baruch, I. S., C. R. Mariaca-Gaspar. A Levenberg-Marquardt Learning Applied for Recurrent Neural Identification and Control of a Wastewater Treatment Bioprocess. – *International Journal of Intelligent Systems*, WILEY Periodicals, Inc., DOI 10.1002/int. 20377, 24, 2009, 1094-1114.

17. Wan, E., F. Beaufays. Diagrammatic Method for Deriving, and Relating Temporal Neural Network Algorithms. – *Neural Computations*, 8, 1996, 182-201.

Manuscript received on 1.11.2011

*Dr. **Ieroham Baruch** obtained his PhD in Technical Sciences for the Higher Mechanical and Electrical Engineering Institute, Sofia, Bulgaria, 1974. Before 1997 he worked as an Associate Professor in the Institute of Engineering Cybernetics and Robotics, Bulgarian Academy of Sciences. After 1997 he joined the Department of Automatic Control, CINVESTAV-IPN, Mexico, working there as a Professor of Automatic Control. His research interests include identification and control of mechanical and biotechnological plants using recurrent neural networks and fuzzy-neural multi-models.*

Contacts:
CINVESTAV-IPN, Department of Automatic Control
Ave. IPN No 2508, Colonia San Pedro Zacatenco, A.P. 14-740, 07360 Mexico D.F.
MEXICO
e-mail: baruch@ctrl.cinvestav.mx

*M. S. E**loy Echeverria Saldierna** received the degree of Engineer in Industrial Robotics from ESIME IPN, Mexico, in 2008, and the M.S. degree in Automatic Control from CINVESTAV IPN, Mexico, in 2011. He is currently a Ph.D. Student in the Department of Automatic Control, CINVESTAV IPN. His research interests are the identification and control of nonlinear dynamic systems and distributed parameter systems using recurrent neural networks.*

Contacts:
Department of Automatic Control, CINVESTAV-IPN, 07360 Mexico D.F., MEXICO

*M. Sc. **Boyka Nenkova** obtained her degrees in 1964 at Sofia University, Faculty of Physics and in 1981 at Technical University, Sofia. Since 1994 she worked in the field of „Recurrent Neural Networks for identification and control of nonlinear plants" as a part of the staff of the Institute for Information Technologies - BAS. After going on pension in 2002 she continued to work in the same field with IICT-BAS and also joining the private company „Risk Engineering" Ltd, working there in other different areas of the energy sector. Her research interests include identification and control of mechanical and biotechnological plants using recurrent neural networks and fuzzy-neural multi-models.*

Contacts:
e-mail: Boyka.Nenkova@RiskEng.bg